The OMEGA Laser Pulse-Shaping System

Laser-fusion experiments require that high-energy, temporally shaped optical pulses be generated and applied to fusion targets. On the OMEGA laser, low-energy optical pulses will be shaped with amplitude modulators and injected into the laser system for amplification and delivery to the laser-fusion targets. A layout of the pulse-shaping system is shown in Fig. 62.14. The output of a single-mode Nd:YLF laser is sliced to produce a 10- to 15-ns square optical pulse. This pulse is sent through two integrated-optic amplitude modulators operated in series and fabricated on a single, fiber-coupled $LiNbO_3$ waveguide. Shaped electrical pulses, synchronized with the input optical square pulse, are applied to the modulators. This shaped optical pulse from the modulators is then preamplified in a regenerative amplifier (regen) and sent to the OMEGA amplifier chains. The shaped electrical pulses are produced using optically activated Si photoconductive (PC) switches and variable impedance microstrip lines. Activation of the Si PC switches is achieved using an optical pulse that has been steepened by the stimulated Brillouin scattering process.

Given the desired optical pulse shape and energy on target, the required output optical pulse shape from the modulator is determined by modeling the temporal pulse distortions introduced by the OMEGA laser system from all sources and then using this model as a transfer function to relate the input to output pulse shapes from the system. This model, available in the form of a computer code (*RAINBOW*), takes into account such factors as the effects of the frequency-tripling process and gain saturation in the amplifiers. Since the optical transfer function of a modulator is well known in terms of the voltage waveform applied to the modulator, a knowledge of the optical pulse shape required on target uniquely determines the required voltage waveform that must be applied to the modulator.

Optical Modulators

A schematic of a typical dual-amplitude, fiber-coupled, waveguide integrated-optic modulator is shown in Fig. 62.15. The input and output fibers are single-mode polarization-preserving fiber with industry-standard FC/APC connectors. Light launched into the input fiber is coupled into a waveguide in the $LiNbO_3$ electro-optic crystal. A Y-branch is used to split the signal and form two arms of a Mach-Zehnder interferometer. Electrodes are placed around the interferometer arms so that a voltage applied to the RF port produces a phase shift in each arm of the interferometer. The polarity of these electrodes is arranged such that the device operates in a push-pull fashion,

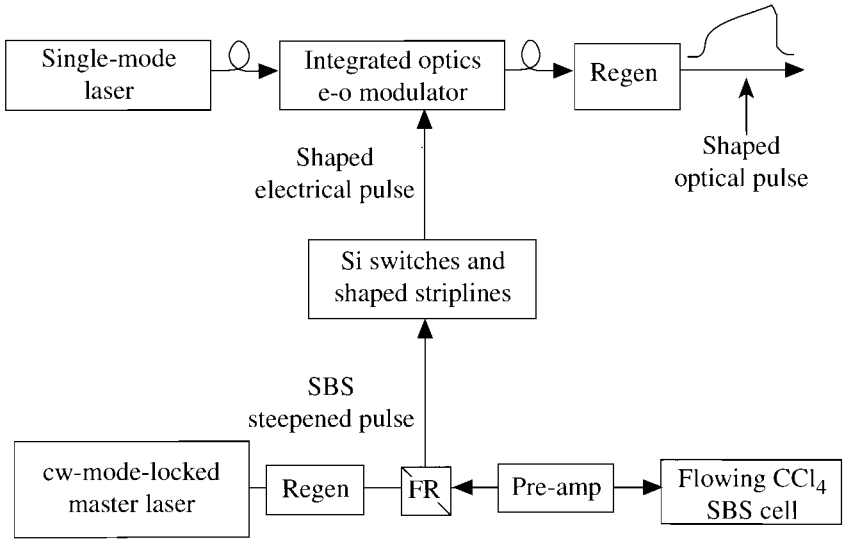

E7021

Figure 62.14
A block diagram of the OMEGA optical-pulse-shaping system. The electrical-pulse-generation portion of the system uses Si photoconductive switches that are activated with an SBS-steepened optical pulse.

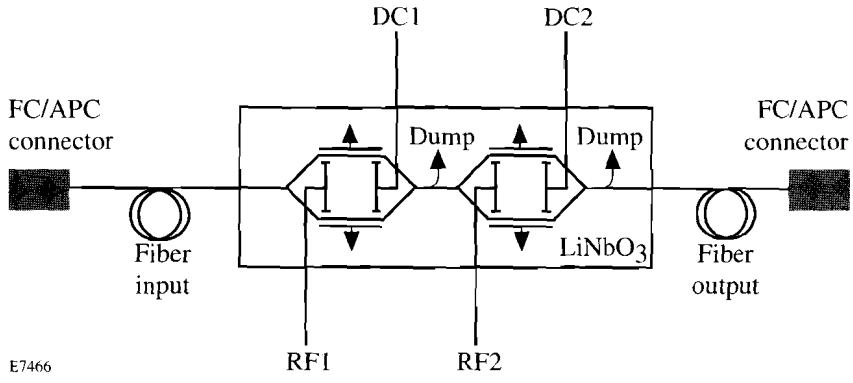

Figure 62.15
The dual-amplitude, Mach-Zehnder, waveguide integrated-optic modulator used for pulse shaping. Shaped voltage waveforms are applied to the RF input ports, and each modulator has a DC input port for setting the dc offset.

i.e., the phase shift in the two arms is cumulative. A second Y-branch is used to coherently combine the two beams and send the shaped pulse to the next stage, while the unwanted radiation is sent to an appropriate beam dump. The device incorporates two identical modulators in series. The output optical pulse intensity from a modulator is given by

$$I(t) = I_0(t)\cos^2\left[\frac{\pi}{2}\frac{V(t)}{V_\pi} + \phi\right], \qquad (1)$$

where $I_0(t)$ is the input optical pulse intensity to the modulator, $V(t)$ is the applied voltage, V_π is the half-wave voltage [the voltage required to drive the modulator from its maximum to its minimum transmission (<10 V)], and ϕ is an overall phase that can be controlled by an applied 0- to 10-V dc bias (provided by a computer with an A/D board). In our case, the input optical pulse to the modulator is a square optical pulse (~10-ns FWHM) obtained by "slicing out" the center of a single-longitudinal-mode Nd:YLF laser pulse (pulsewidth ~100-ns FWHM) using conventional Pockels cells. The modulators are designed for 1054-nm-wavelength operation and have traveling wave electrodes to provide an 8-GHz bandwidth.

Electrical Waveform Generation

To produce shaped optical pulses from the modulators, temporally shaped voltage waveforms [$V(t)$ in Eq. (1)] must be applied to the modulators. (The modulator is dc biased so that $\phi = \pi/2$.) The electrical-pulse-generation system that shapes the voltage waveforms applied to the modulators is modeled after a design developed at Lawrence Livermore National Laboratory (LLNL).[1] The system consists of two Si PC switches, a microstrip charge line, and a variable impedance microstrip line as shown in Fig. 62.16. The microstrip charge line is placed between two PC switches and is charged to approximately 80 V. The opposite side of one PC switch is connected to the modulator, while the opposite side of the other PC switch is connected to the terminated variable-impedance microstrip line. When the PC switch near the variable-impedance microstrip line is activated (closed), a square pulse is sent to the

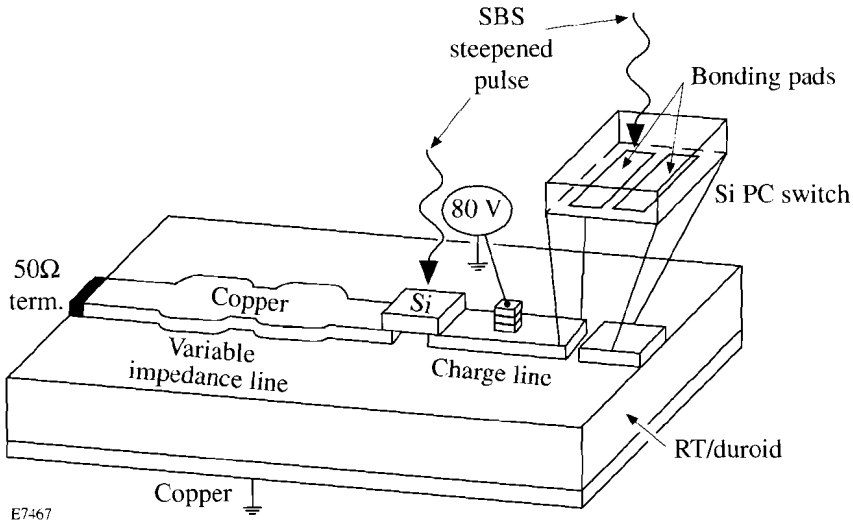

Figure 62.16
A detailed view of the electrical-pulse-generation system consisting of two optically activated Si PC switches, a microstrip charge line, and a terminated variable-impedance microstrip line.

variable-impedance microstrip line. A voltage waveform is then reflected from the variable-impedance line with a specific shape depending on the impedance mismatches along the length of the line. This shaped voltage waveform propagates back through the PC switch and charge line toward the modulator. Just before the waveform reaches the modulator PC switch, this switch is activated, allowing the voltage waveform to be applied to the RF input port of the modulator. The exact shape of the voltage waveform can be controlled by the judicious placement of impedance variations along the length of the variable-impedance microstrip line.

The system of microstrip lines and switches is designed to be impedance matched to the 50-Ω input impedance of the modulators and test equipment used. Microstrip lines were chosen instead of strip lines to minimize the impedance mismatch at the Si switches. The charge line and variable-impedance microstrip lines are fabricated in 0.79-mm-thick RT/duroid 5880 microwave laminate having 36-μm-thick Cu on both sides. An impedance variation along the line is obtained by adjusting the width of the top Cu electrode. The exact geometry is easily calculated knowing the required voltage waveform that must be produced. The reflection coefficient along the line can be calculated using a layer-peeling technique.[2] The impedance as a function of position along the line is then obtained from the reflection coefficient along the line. Finally the width of the electrode along the line is calculated using simple relationships between the material parameters and the impedance variations.[3] To fabricate the microstrip line, the Cu material on one side is machined with a precision programmable milling machine to produce the desired width as a function of length. The charge line is a constant 50-Ω microstrip line (Cu width = 2.38 mm) with a 2-mm gap at both ends to facilitate Si switch mounting. The Si switches, 2 mm long by 2.38 mm wide (to match the width of the 50-Ω charge line) by 0.5 mm thick, have bonding pads with 1-mm separation. The switches are low temperature soldered across each gap in the charge line with the bonding pads facing the Cu of the microstrip line, as shown in Fig. 62.16. The switches are illuminated from the back (opposite side from the contact pads) using 1054-nm laser radiation with ~0.5 mJ of energy per pulse. The laser radiation is absorbed throughout the entire volume of the 0.5-mm-thick Si switch, which results in switch activation. When illuminated with a laser pulse, the switch resistance changes from its dark value of approximately 600 kΩ to its activated resistance of less than 1 Ω as the absorbed photons generate electron hole pairs in the Si and reduce the resistivity of the material.

The square pulse sent to the variable-impedance microstrip line must contain frequency components high enough to reflect the pulse shapes of interest. Photoconductive switches can be activated (closed) in a time comparable to the rise time of the activating optical pulse (<100 ps), which in this case is a pulse that has its leading edge steepened by the stimulated Brillouin scattering (SBS) process. A typical square pulse produced by activating one switch only is shown in Fig. 62.17. The rising edge of the electrical pulse is approximately 80 ps, as measured with a Tektronix 7250 oscilloscope (~10-GHz bandwidth).

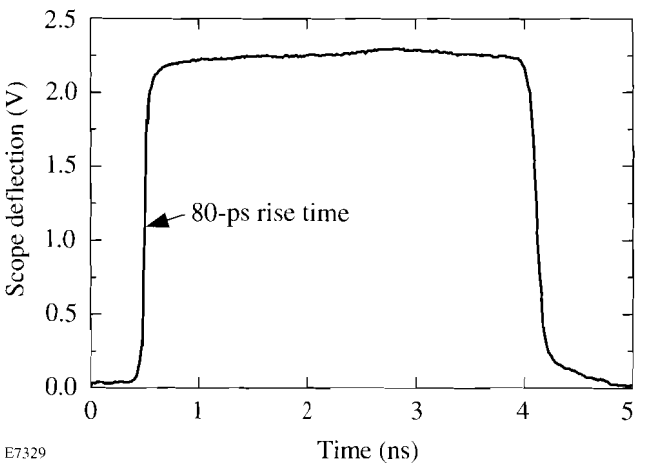

Figure 62.17
A square electrical pulse generated by the charge line and a Si PC switch. The pulse has a rise time of approximately 80 ps.

High bandwidth must be maintained throughout the entire system. High-bandwidth SMA end launchers and cables are used to transfer the electrical pulses from the microstrip line to the modulator or test equipment being used. Care is taken to minimize the impedance mismatch in the charge line at the point where the charging voltage is applied; this is done by charging through three board-mounted chip resistors (~10 kΩ each) stacked in series, as shown in Fig. 62.16. Less than 0.6% reflection at 10 GHz is produced by this process, as determined from time-domain reflectometer (TDR) measurements. A TDR of the complete microstrip line can be taken by soldering copper strips across the gaps in place of the Si switches. Figure 62.18 shows (1) the TDR measurement of a variable impedance microstrip line (taken with a 20-GHz-bandwidth HP 5420B TDR oscilloscope) with Si switches removed, compared to the design shape, and (2) the shaped electrical pulse transferred into the Tektronix 7250 oscilloscope after passing through the two Si switches that have been activated as described above. From Fig. 62.18 we see that, although the

present Si switches clearly degrade the inherent frequency response of the system, high-bandwidth shaped electrical pulses can ultimately be achieved with this pulse-generating system. Research is continuing in this area to improve the overall system performance.

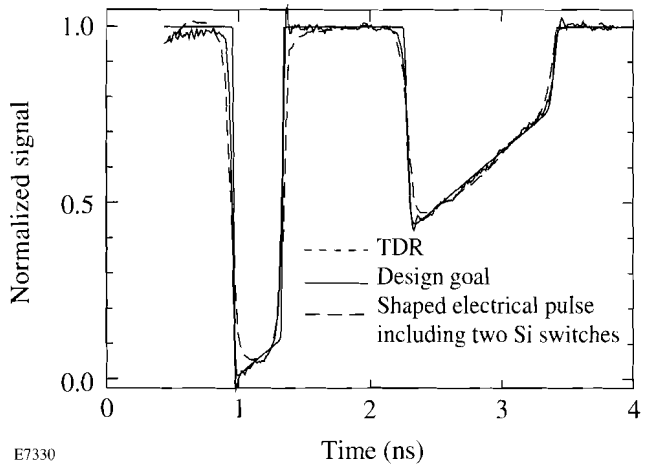

Figure 62.18
Time-domain reflectometer (TDR) measurement of a variable impedance microstrip line (dotted line) compared to the design goal (solid line). The dashed line is the measured shaped electrical pulse after propagation through two Si PC switches.

PC Switch Activation

To produce fast closing times the PC switches must be activated by illuminating them with optical energy in as short a time as possible. Once the switches are closed, they must stay closed for a long time in comparison to the desired electrical pulse shapes of interest (~10 ns). Silicon PC switches were chosen for this application because of their long recombination times (100 to 200 μs). The switches are activated with fast-rise-time, high-contrast optical pulses generated by the SBS process.[4–5] The experimental setup is shown in Fig. 62.14.

A 1054-nm, 1- to 3-ns FWHM pulse (controlled by intracavity etalons[6]) from a Nd:YLF regen is amplified to 3 to 5 mJ and focused into a liquid cell containing carbon tetrachloride (CCl_4). A Brillouin-Stokes pulse is generated in the backward direction from this cell due to the SBS process. The SBS process is an intensity-dependent, nonlinear process where the incident laser Bragg-scatters in the backward direction from a driven acoustic wave in the medium. The process can be modeled as a pure gain process whereby a backward-traveling Brillouin noise signal experiences exponential-type gain throughout the focal region of the laser and grows into the Brillouin-Stokes signal. The gain coefficient depends on the laser intensity and the response time of the Brillouin medium (less than 1 ns for CCl_4).[7] The low intensity at the beginning of the laser pulse is transmitted through the cell, with little energy converted to the Brillouin signal. As the laser intensity in the cell increases during the laser pulse, the cell begins to generate Brillouin Stokes energy very rapidly due to the nonlinear buildup of the acoustic wave. The process quickly saturates, after which the laser scatters into the Stokes wave with high efficiency. The backscattered Brillouin pulse from the SBS cell has a fast-rising edge (<100-ps measurement limited) due to this Brillouin pulse steepening, while the back of the pulse approximates that of the laser. The reflected Brillouin pulse is sent back through the preamplifier and switched out using polarization optics and a Faraday rotator (FR). The SBS pulse is then split and used to activate both PC switches by introducing an appropriate timing delay between the two pulses.

Typical SBS reflected pulses for different incident laser energies are shown in Fig. 62.19. As the incident laser energy is varied, the location in time of the fast-rising edge of the SBS pulse changes. As seen in Fig. 62.19, as we increase (decrease) the laser energy, the SBS process turns on earlier (later). Hence, amplitude fluctuations in the laser may result in timing jitter of the electrical-pulse-generation system. To obtain electrical waveforms from the pulse-generation system that are

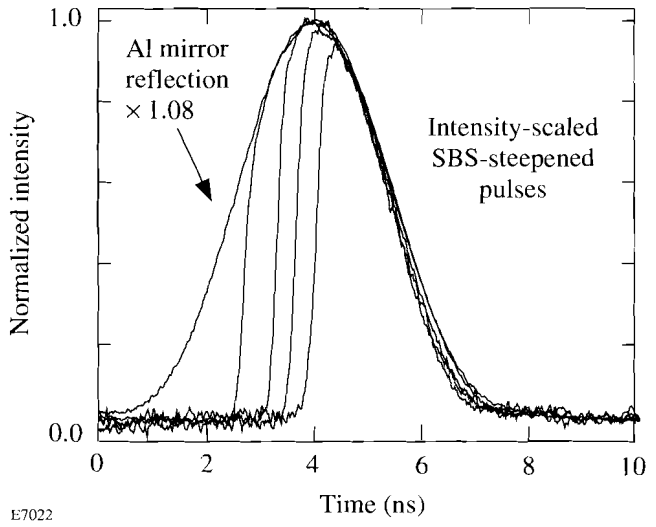

Figure 62.19
Fast-rise-time optical pulses produced by SBS pulse steepening with varying laser input energy. As the incident laser energy is increased (decreased), the SBS pulse turns on earlier (later). The reflected SBS pulse has a rise time of less than 100 ps.

accurately synchronized to a master timing reference, the laser that activates the PC switches must be amplitude stable. The laser amplitude in our setup is actively stabilized to within 3% using an optical feedback system that controls the cavity losses during the pulse build-up phase. A shaped optical pulse from the pulse-shaping system (including the Si PC switches, variable-impedance microstrip line, optical modulator, and regen preamplifier) was produced, and the shot-to-shot timing jitter between the shaped optical pulse and the master cw-mode-locked laser pulse injected into the regen that activates the PC switches was measured. An absolute timing jitter of less than 30 ps was measured using the Tektronix 7250 oscilloscope (~10-GHz bandwidth) and fast detectors (~3.5-GHz bandwidth).

The SBS process has an additional advantage when using Si PC switches. The SBS process is nonlinear, and for low incident laser energy into the SBS cell, essentially no Brillouin energy is reflected; hence, all laser prepulse noise is eliminated, resulting in a very-high on/off contrast ratio. This is important for Si switch applications because the recombination times are long (100 to 200 μs) and the switch will integrate the incident energy during this recombination time. Elimination of all prepulse optical noise ensures proper switch performance.

System Performance

Optical pulses have been produced with the pulse-shaping system described above. Figure 62.20 shows an optical pulse shape produced by the system (solid line). To produce this shape, a square optical pulse (~10-ns FWHM) is used as input to the modulator. This pulse is obtained by slicing out the center of a single-longitudinal-mode Nd:YLF laser pulse (pulse width ~100-ns FWHM) using conventional Pockels cells, as was mentioned previously. The square pulse is then transferred to the modulator through optical fibers. Synchronized with this optical pulse is the electrical pulse (Fig. 62.18) that was produced by the electrical pulse generator described above. Figure 62.20 also shows the optical pulse shape expected from the modulator (dashed line) if the design goal of Fig. 62.18 is substituted into the modulator transfer function [Eq. (1)], and the optical pulse shape expected from the modulator (dotted line) if the measured shaped electrical pulse of Fig. 62.18 is substituted into the modulator transfer function [Eq. (1)].

The optical pulse in Fig. 62.20 was measured at the output of the modulator with a 25-GHz bandwidth detector (New Focus 1414). The energy at this point in the pulse-shaping system is approximately 10 nJ per pulse and is too low to make temporal measurements of a single pulse. The measurement

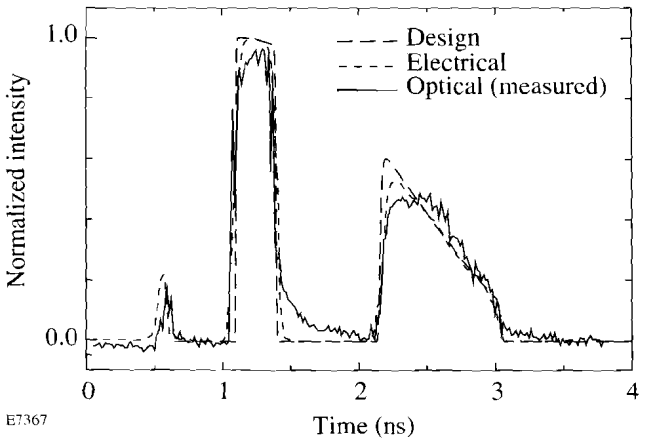

Figure 62.20
A comparison of expected and observed optical pulse shapes from the OMEGA laser's pulse-shaping system. Actual measured optical pulse shape from the modulator (solid line); optical pulse shape expected from the modulator if the design goal of Fig. 62.18 is substituted into the modulator transfer function [Eq. (1)] (dashed line); optical pulse shape expected from the modulator if the measured shaped electrical pulse of Fig. 62.18 is substituted into the modulator transfer function [Eq. (1)] (dotted line).

was taken with a high-bandwidth sampling oscilloscope (HP 5420B) and includes averaging over many pulses. The optical pulse shape in Fig. 62.20 appears to deviate from the expected pulse shape. We believe that the deviations are largely due to the detector response. In fact, our measurements show that large discrepancies occur between high-bandwidth detectors when measuring the same optical pulse. These detectors are designed to measure short pulses with fast rise times but have varying responses when trying to measure long pulses with fast rising structure. Work is continuing in this area to make accurate measurements of these shaped pulses. A streak camera will be used to measure these pulses and is expected to provide more accurate results.

In summary, an optical-pulse-shaping system has been designed that is capable of meeting the future pulse-shaping requirements for the OMEGA laser. The system has been tested and is capable of producing shaped optical pulses with 50- to 100-ps structure over a several-nanosecond pulse envelope.

ACKNOWLEDGMENT

This work was supported by the U.S. Department of Energy Office of Inertial Confinement Fusion under Cooperative Agreement No. DE-FC03-92SF19460, the University of Rochester, and the support of the Frank Horton Graduate Fellowship Program. The support of DOE does not constitute an endorsement by DOE of the views expressed in this article.

REFERENCES

1. R. B. Wilcox *et al.*, in *Laser Coherence Control: Technology and Applications*, edited by H. T. Powell and T. J. Kessler (SPIE, Bellingham, WA, 1993), Vol. 1870, pp. 53–63.
2. S. C. Burkhart and R. B. Wilcox, IEEE Trans. Microw. Theory Tech. **38**, 1514 (1990).
3. B. C. Wadell, *Transmission Line Design Handbook* (Artech House, Boston, 1991).
4. T. de Saxce and P. Picart, in *Optically Activated Switching III*, edited by R. A. Falk (SPIE, Bellingham, WA, 1993), Vol. 1873, pp. 262–271.
5. A. Okishev, M. D. Skeldon, and W. Seka, in *CLEO '94, 1994 Technical Digest Series, Volume 8*, Anaheim, CA, 8–13 May 1994, paper CTuQ5.
6. M. D. Skeldon and S. T. Bui, J. Opt. Soc. Am. B **10**, 677 (1993).
7. W. Kaiser and M. Maier, in *Laser Handbook*, edited by F. T. Arecchi and E. O. Schulz-Dubois (North-Holland, Amsterdam, 1972), Vol. 2, p. 1077.